Journal of Statistical Physics, Vol. 32, No. 3, 1983

Van Hove Self-Correlation Function of a Hard-Disk Fluid: Enskog Theory and Computer Simulation

E. Leutheusser,[1,2] D. P. Chou,[1,3] and Sidney Yip[1]

Received January 11, 1983

The van Hove self-correlation function in a hard-disk fluid is analyzed using the Lorentz–Enskog kinetic equation and the kinetic model method of solution. Numerical convergence of the model solutions is demonstrated and accurate model results are used to interpret molecular dynamics simulation data at finite wave numbers. It is found that at about 60% of freezing density the error in the Enskog theory can be mainly attributed to an underestimate of the effective self-diffusion coefficient, but at 90% freezing density a theory which treats correlated collisions is needed to describe the width behavior of the single-particle density fluctuation spectrum.

KEY WORDS: Hard-disk fluid; Lorentz–Enskog kinetic equation; kinetic model solution; van Hove self-correlation function; molecular dynamics results; self-diffusion coefficient.

1. INTRODUCTION

The dynamics of single particle motions in a simple fluid is described by the van Hove self-correlation function $G_s(r,t)$ which is the time-dependent spatial distribution of a tagged particle.[1] While $G_s(r,t)$ is related to the velocity autocorrelation function $\phi_{vv}(t)$, a knowledge of $\phi_{vv}(t)$ is not sufficient to completely determine $G_s(r,t)$. Thus, through G_s one has the possibility of studying spatial correlation effects not directly present in $\phi_{vv}(t)$ or its time integral, the self-diffusion coefficient D.

[1] Department of Nuclear Engineering, Massachusetts Institute of Technology, Cambridge, Massachusetts 02139.

[2] Feodor Lynen Stipendiat of Alexander von Humboldt-Stiftung, on leave of absence from Physik-Department, Technische Universität München, D-8046 Garching, West Germany.

[3] Present address: Institute of Nuclear Energy Research, P.O. Box 3-10, Lung Tan, Taiwan 325.

0022-4715/83/0900-0523$03.00/0

The hard-disk fluid plays an important role in the theory of liquids and gases ever since the discovery of the nonexponential long-time decay of time correlation functions.[2] For this system the velocity autocorrelation function has been studied extensively by molecular dynamics simulation,[2,3] and considerable theoretical analysis also has been carried out.[4,5] On the other hand, there exists no theoretical discussion or computer simulation data on the self-correlation function of a hard-disk fluid in the literature.

The purpose of this paper is to investigate the Enskog kinetic theory description of the self-correlation function. This description is expected to be a good approximation in the experimentally accessible time and wavenumber regimes at moderate fluid densities, but at sufficiently high density it is expected to break down because the effects of correlated collisions will become important and these are not treated in the Lorentz–Enskog kinetic equation. We first consider the kinetic model method of analyzing the kinetic equation and examine the accuracy of a single relaxation time approximation. Then by comparing the numerical solutions with new molecular dynamics simulation data, we are able to delineate the limitations of the Lorentz–Enskog theory at high densities. In a separate work we have carried out a similar study of the density fluctuations and related space-dependent time correlation functions and have found the generalized Enskog kinetic equation to be valid up to at least $A/A_0 = 3$, where A is the area of the fluid system and A_0 is the area at close packed.[6] The conclusion which emerges from both studies is that the Enskog theory is valid at densities up to about half the solidification density, and that for more dense fluids a theory which also treats dynamically correlated collisions is needed.

2. KINETIC, EQUATION AND SOLUTION

We consider a system of hard disks of diameter σ and mass m at a density n. We are interested in the dynamical properties of a tagged particle whose position and momentum will be donated by $\mathbf{r}_0$ and $\mathbf{p}_0$, respectively. Its phase-space correlation function is defined as

$$\phi(12,t) = (f(1,t)\,|\,f(2)) \tag{1a}$$

where $f(1) = \delta(\mathbf{r} - \mathbf{r}_0)\delta(\mathbf{p} - \mathbf{p}_0)$ is the phase space density, and the bracket denotes an equilibrium average $(A\,|\,A) = \langle \delta A^* \delta A \rangle$ of the fluctuation $\delta A = A - \langle A \rangle$. The Fourier and Laplace transform of $\phi(12,t)$ is defined by

$$\phi_{\mathbf{pp}'}(q,z) = i\int_0^\infty dt\, e^{izt} \int d\mathbf{r}_{12}\, e^{-i\mathbf{q}\cdot\mathbf{r}_{12}} \phi(12,t), \qquad \mathrm{Im}\, z > 0 \tag{1b}$$

The correlation function ϕ obeys a kinetic equation which may be derived

in a similar way as before[6]:

$$\left[(z - \mathbf{q}\cdot\mathbf{v})\delta_{\mathbf{p}\bar{\mathbf{p}}} + C_{\mathbf{p}\bar{\mathbf{p}}}(\mathbf{q},z)\right]\phi_{\bar{\mathbf{p}}\mathbf{p}'}(q,z) = -\chi_{\mathbf{p}\mathbf{p}'} \tag{2a}$$

The equal time phase-space correlation $\chi_{\mathbf{p}\mathbf{p}'} = \varphi(p)\delta_{\mathbf{p}\mathbf{p}'}$ is given in terms of the Maxwellian velocity distribution $\varphi(p) = (2\pi mT)^{-1}\exp(-p^2/2mT)$. The effects of particle interactions are described by the generalized collision operator $C_{\mathbf{p}\mathbf{p}'}(\mathbf{q},z)$, which has two parts of different physical significance:

$$C_{\mathbf{p}\mathbf{p}'}(\mathbf{q},z) = T^s_{\mathbf{p}\mathbf{p}'} + M_{\mathbf{p}\mathbf{p}'}(\mathbf{q},z) \tag{2b}$$

$$T^s_{\mathbf{p}\mathbf{p}'} = -ig(\sigma)n\sigma\int d\hat{r}\int d\mathbf{p}_0\, d\mathbf{p}_1\,\varphi(p_0)\varphi(p_1)\theta(\mathbf{v}_{01}\cdot\hat{r})(\mathbf{v}_{01}\cdot\hat{r})$$
$$\times\delta(\mathbf{p}-\mathbf{p}_0)\left[\delta(\mathbf{p}'-\mathbf{p}_0^*) - \delta(\mathbf{p}'-\mathbf{p}_0)\right] \tag{2c}$$

The Lorentz–Enskog operator $T^s_{\mathbf{p}\mathbf{p}'}$ describes uncorrelated binary collisions while $M_{\mathbf{p}\mathbf{p}'}(\mathbf{q},z)$ accounts for collision sequences involving more than two particles. In Eq. (2c) $\mathbf{p}_0^* = \mathbf{p}_0 - (\mathbf{p}_{01}\cdot\hat{r})\hat{r}$ is the momentum of the tagged particle after the collision, $\hat{r} = \mathbf{r}/|\mathbf{r}|$ denotes a unit vector and $g(\sigma)$ is the pair correlation at contact.

An exact expression may be written down for $M_{\mathbf{p}\mathbf{p}'}(\mathbf{q},z)$, but we will not need it here. Instead, we are interested in the solution of the approximate kinetic equation, the Lorentz–Enskog equation, which is obtained from Eq. (2) by dropping $M_{\mathbf{p}\mathbf{p}'}(\mathbf{q},z)$ completely. Note that Eq. (2) differs from the generalized Enskog kinetic equation discussed elsewhere[6] in that there is no mean-field term in $C_{\mathbf{p}\mathbf{p}'}$ and the equal-time correlation $\chi_{\mathbf{p}\mathbf{p}'}(\mathbf{q})$ is simpler. Also, the binary collision operator is not only frequency independent due to the instantaneous nature of hard-core collisions, but also wave number independent.

To solve the kinetic equation, Eq. (2), the kinetic model method is employed.[7] A complete orthonormal set of momentum states $|k\rangle$, $k = 1, 2, \ldots,$ is chosen and the infinite-dimensional collision operator matrix $C_{ik}(\mathbf{q},z)$ is replaced by a finite $N\times N$ matrix with the remainder approximated by a single diagonal element $C_{ik}(\mathbf{q},z) = \alpha(q,z)\delta_{ik}$ for $i,k > N$, with $\alpha(q,z) = \langle N+1|C(\mathbf{q},z)|N+1\rangle$. Then Eq. (2) may be solved easily and one obtains the $N\times N$ matrix equation

$$\phi(q,z) = \left[1 - \gamma(q,z)\phi^{(0)}(q,z')\right]^{-1}\phi^{(0)}(q,z') \tag{3}$$

Here, $\phi^{(0)}(q,z)$ denotes the matrix of free particle correlations $\phi^{(0)}_{ik}(q,z) = \langle i|(\mathbf{q}\cdot\mathbf{v} - z)^{-1}|k\rangle$, $z' = z + \alpha(q,z)$ and $\gamma_{ik}(q,z) = C_{ik} - \alpha(q,z)\delta_{ik}$. The set of momentum functions $|k\rangle$, the general matrix elements of the Lorentz–Enskog operator, and the free-particle propagators are given explicitly in the Appendix. Note that by increasing N the approximate solution Eq. (3) will converge to the exact solution of the kinetic equation,

Eq. (2). The rate of convergence will be shown numerically later. The kinetic model formulation also ensures that the correct free-particle limit is obtained.

We are particularly interested in the incoherent dynamic structure factor or the van Hove self-correlation function, $S_s(q,\omega)$, which is the spectrum of density fluctuations of the tagged particle $S_s(q,\omega) = \phi''_{11}(q,\omega)$ where the state $|1\rangle = 1$ denotes the density state and $\phi_{11}(q,\omega \pm i0) = \phi'_{11}(q,\omega) \pm i\phi''_{11}(q,\omega)$. Its Fourier transform is the intermediate scattering function $F_s(q,t)$ which can be generated by molecular dynamics simulation.

We will first discuss several limiting cases. For the noninteracting system the density correlation function is $\phi^{(0)}_{11}(q,z) = (\pi/2)^{1/2}(qv_0)^{-1} w(z/\sqrt{2}\, qv_0)$, where $w(x)$ is the plasma dispersion function and $v_0 = (T/m)^{1/2}$ is the thermal velocity. This limit will be approached at large wave numbers. The spectrum in this case is a Gaussian with half-width at half maximum $\omega_{1/2}(q) = \sqrt{2}\, qv_0(\ln 2)^{1/2}$. On the other hand, because of particle number conservation, one expects diffusive behavior for small wave numbers. It is then convenient to define a generalized diffusion constant $D(q,z)$ by

$$\phi_{11}(q,z) = -\frac{1}{z + q^2 D(q,z)} \tag{4}$$

The zero wave number limit of $D(q,z)$ is related to the velocity autocorrelation function

$$\phi_{vv}(z) = i\int_0^\infty dt\, e^{izt}(v_y(t)\,|\,v_y) = \lim_{q\to 0} D(q,z) \tag{5}$$

The zero-frequency limit defines the diffusion constant D by $\lim_{z\to 0}\phi_{vv}(z) = iD$, if the limit exists. If D is finite then the density fluctuation spectrum at small wave numbers is a Lorentzian with width $\omega_{1/2}(q) = Dq^2$. This is the case for the solution of the Lorentz–Enskog equation.

One can also define a velocity relaxation kernel $K(z)$ by

$$\phi_{vv}(z) = -\frac{v_0^2}{z + K(z)} \tag{6}$$

In first approximation one finds from Eq. (2a) $K(z) = i\nu$, where $\nu = 2\sqrt{\pi}\, n\sigma v_0 g(\sigma)$ is the collision frequency. Thus, the single relaxation time approximation gives $D_0 = v_0^2/\nu$. From Eq. (6) the corresponding $\phi_{vv}(t)$ is a single exponential.[8] In general, $K(z)$ for the Lorentz–Enskog equation will be frequency dependent since the velocity state is not an eigenfunction of the collision operator. But the frequency dependence is quite weak; for

example, in the second approximation one finds

$$K(z) = i\nu + \frac{\nu^2/32}{z + i\nu(43/32)} \tag{7}$$

For the diffusion constant this implies $D/D_0 = 1.024$, while the exact result is $D/D_0 = 1.02709\ldots$. In the nth approximation $\phi_{vv}(t)$ is a sum of n exponentials. The $n = 5$ result has been given explicitly in the literature[3] and may be considered to be a sufficiently accurate solution of the Lorentz–Enskog equation for all purposes.

We will not discuss the density fluctuation spectrum in the single relaxation time approximation. It may be written in the form of Eq. (4) with $D(q,z)$ replaced by its free-particle approximation $D(q,z) = D^{(0)}(q, z')$ with $z' = z + i\nu$.[9] It is a reasonable interpolation between the free-particle limit at large wave numbers and the hydrodynamic limit discussed above at small wave numbers. Furthermore, in order to reproduce the correct diffusion constant D, the single relaxation time model can be modified by replacing ν by $\nu \cdot D_0/D$. This approximation will be referred to as the Nelkin–Ghatak (NG) model.[8]

The short time expansion of $F_s(q,t)$ for a hard-disk fluid is known up to the t^4-term

$$F_s(q,t) = 1 - \frac{1}{2}(qv_0t)^2 + \frac{1}{3!}(qv_0t)^2(\nu t) - \frac{1}{4!}(qv_0t)^2\left[a(\nu t)^2 - 3(qv_0t)^2\right] + \cdots \tag{8a}$$

The first three terms are reproduced exactly by the Lorentz–Enskog equation. For the collisional part of the fourth term, the single relaxation time approximation yields $a_{SR} = 1$, while the exact solution[10] to the Lorentz–Enskog equation gives $a_E = 1.0316\ldots$. In general, the coefficient a involves the static three-particle correlation; the numerical result at low density is $a = 1.0386\ldots$.[10] The short time expansion of the velocity autocorrelation function is correspondingly

$$\phi_{vv}(t) = 1 - \nu t + \tfrac{1}{2}a(\nu t)^2 + \cdots \tag{8b}$$

Since $\phi_{vv}(t)$ has recently been studied extensively,[3] we will not discuss it further here.

3. MOLECULAR DYNAMICS SIMULATION

A molecular dynamics program for the simulation of hard-disk and hard-sphere fluids has been developed[11] which is a modified version of the program constructed by Prueitt.[12] Equation of state data for both two

Table I. Effective Self-Diffusion Coefficients of Hard-Disk Fluids

A/A_0	$D\tau/\sigma^2$	$D/D_0{}^a$
5.0	0.866	1.09
2.0	0.041	1.16
1.4	0.0029	0.775

[a] $D_0 = [2n\sigma g(\sigma)(\pi m/T)^{1/2}]^{-1}$.

and three dimensions were generated which are in agreement with the published results.[13] For hard disks the static structure factor $S(q)$ was calculated at two densities, $n^* = n\sigma^2 = 0.578$ ($A/A_0 = 2$) and 0.825 ($A/A_0 = 1.4$), and selected values of wave number. Also, for hard disks the velocity autocorrelation function and the mean square displacement $\langle r^2(t)\rangle$ were calculated at $n^* = 0.231$, 0.578, and 0.825. Since our interest was not in the long-time behavior, no attempt was made to obtain data beyond the intermediate-time domain, $t > 10$–20τ for $\phi_{vv}(t)$ and $t > 50\tau$ for $\langle r^2(t)\rangle$, where $\tau = 1/\nu$ is the Enskog mean collision time. We do not present the

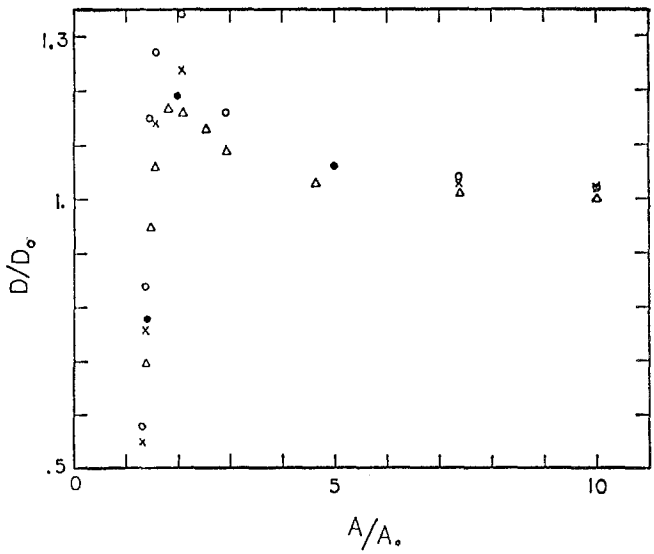

Fig. 1. Density dependence of effective self-diffusion coefficient in a hard-disk fluid. D_0 is Enskog diffusion coefficient, and $n\sigma^2 = (2/\sqrt{3})(A/A_0)^{-1}$. Present molecular dynamics data are shown as closed circles. Other data, $N = 108$ (triangles), $N = 500$ (crosses), and infinite system extrapolation (open circle), are obtained by converting the three-dimensional molecular dynamics data[14] using the relation $A/A_0 = (V/V_0)^{2/3}$.

results here since much more extensive and precise data have now been published.[3] It is interesting to remark, however, that the $\langle r^2(t)\rangle$ data show a well-established linear behavior so that one can readily deduce an *effective* self-diffusion coefficient D_{eff} from its slope, or equivalently[14]

$$D_{\text{eff}} = \frac{1}{4}\frac{d}{dt}\langle r^2(t)\rangle \tag{9}$$

We refer to the diffusion coefficient as D_{eff} because the Green–Kubo expression for D diverges in two dimensions.[2–5] The values obtained from the present data are shown in Table I. It should be pointed out as a purely empirical observation that these values are quite consistent with the hard-sphere data in the literature,[14] as shown in Fig. 1, if one simply scales the density according to $A/A_0 = (V/V_0)^{2/3}$, where V is the fluid volume and V_0 the volume at close packed.

Using the simulation trajectories at $A/A_0 = 2$ and 1.4, we have generated the intermediate scattering function $F_s(q,t)$ at several q values. These will be compared to the kinetic model solutions in the next section to delineate more precisely the way in which Enskog theory breaks down at high densities.

4. RESULTS AND DISCUSSIONS

To obtain numerical results from the Lorentz–Enskog kinetic equation one need only specify the pair correlation function at contact $g(\sigma)$. We will use the empirical expression[15]

$$g(\sigma) = \frac{1 - 7\zeta/16}{(1-\zeta)^2} - \frac{\zeta^3/64}{(1-\zeta)^4} \tag{10}$$

Table II. Convergence of Kinetic Model (Order N) Solutions for $S_s(q,\omega)$ for a Hard-Disk Fluid, $A/A_0 = 2$ and $q\sigma = 4$

N	Δ_N[a]
2	7.9
5	−2.1
9	−0.7
14	−0.2
20	−0.06

[a] $\Delta_N \equiv [S_s(q,\omega=0)_N - S_s(q,\omega=0)_{N=27}] \times 100/S_s(q,\omega=0)_{N=27}$ is the maximum deviation (expressed in percent) from the $N = 27$ kinetic model solution.

where $\zeta = (\pi/4)n\sigma^2$ is the packing fraction, which agrees well with Monte Carlo results. For a demonstration of the accuracy of the kinetic model solution the dynamic structure factor $S_s(q,\omega)$ at $A/A_0 = 2$ has been evaluated using kinetic models of various order N. Table II shows the convergence of the low-order solutions for the peak height of $S_s(q,\omega)$ at an

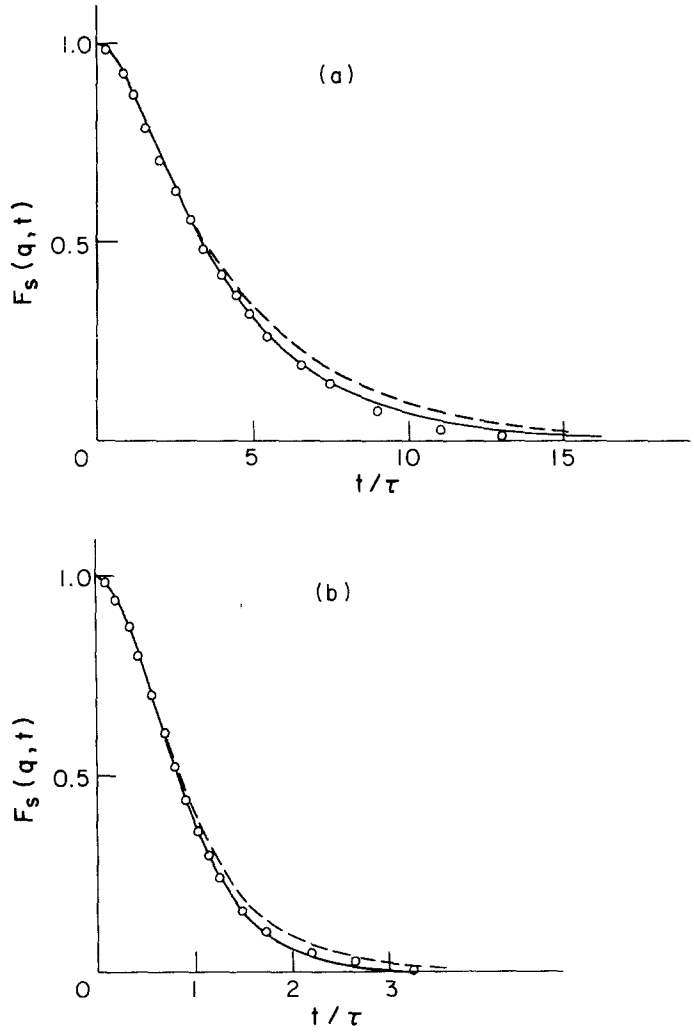

Fig. 2. The van Hove self-correlation function $F_s(q,t)$ in a hard-disk fluid ($A/A_0 = 2$), $N = 27$ kinetic model solution (full curve), single relaxation time approximation (dashed curve), and molecular dynamics simulation data (circles). (a) $q\sigma = 3$. (b) $q\sigma = 9$. τ is Enskog mean collision time.

intermediate value of dimensionless wave number $q\sigma$ since the deviations are smaller at small and large q. In Table II the model result for $N = 27$ was assumed to be numerically converged. From this comparison one may conclude that the kinetic model with $N = 9$ should be everywhere accurate to within 1% of the converged solution.

We consider first the results for $A/A_0 = 2$. The intermediate scattering function $F_s(q,t)$ is shown in Fig. 2 at two values of q. In both cases there is quite good agreement between the molecular dynamics data and the more accurate kinetic model ($N = 9$) solution. It is seen that the short-time behavior is adequately described by any kinetic model, but the intermediate-time decay is sufficiently sensitive to discriminate against the single relaxation time approximation. The deficiency of the Enskog theory in predicting the effective self-diffusion coefficient apparently does not affect appreciably the decay of $F_s(q,t)$. The direct influence of D_{eff} will certainly vary with the density, $q\sigma$ value, and the time domain of decay. One generally expects the effect to be largest at high densities, where D_{eff} deviates significantly from D_0, small $q\sigma$, where hydrodynamic characteristics manifest most strongly, and long times. It is interesting to note that the Nelkin–Ghatak model, which is the single relaxation time approximation combined with scaling the relaxation time to give the correct D, gives results numerically close to the kinetic model solution for $N = 9$. This implies a cancellation of the error associated with the incorrect D value against that associated with the inaccuracy of a low-order kinetic model approximation.

The frequency spectrum $S_s(q,\omega)$ is shown in Fig. 3 for $A/A_0 = 2$ and $q\sigma = 6.1$. Here, it is not so obvious that the more accurate kinetic model solution is in better agreement with the simulation data. This is due at least in part to the incorrect value of D. The importance of D on the line shape can be appreciated by examining the half-width at half-maximum $\omega_{1/2}$, as shown in Fig. 4. There is considerable difference between the NG model and the single relaxation time approximation results, the two models differing only in the value of D, $D_{\text{NG}}/D_0 = 1.19$.

One can expect that at $A/A_0 = 1.4$ the Enskog theory will be considerably less satisfactory than the foregoing results. As shown in Fig. 5, practically the entire decay of $F_s(q,t)$ at $q\sigma = 3$ is sensitive to the value of D_{eff} except for the initial relaxation. As $q\sigma$ increases, there is a noticeable shift to longer times where the effect of D_{eff} is still important ($q\sigma = 11$) until at large wave numbers, for example, $q\sigma = 25$, kinetic effects completely dominate the behavior of $F_s(q,t)$ and there is no longer any influence of D_{eff}.

The deficiency of the Enskog theory becomes apparent when the width of $S_s(q,\omega)$ is considered at $A/A_0 = 1.4$. Figure 6 shows the simulation data

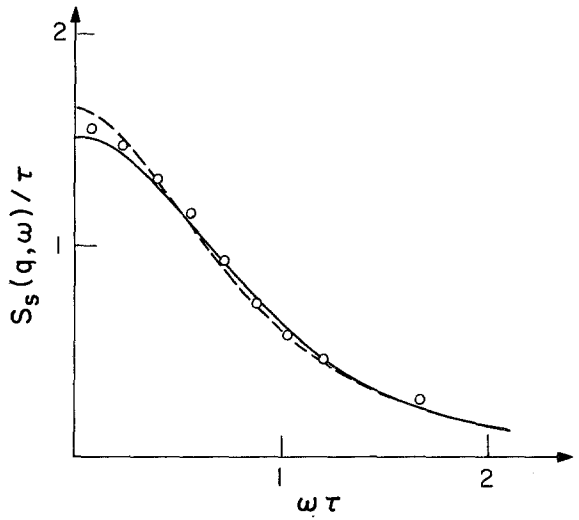

Fig. 3. Single-particle density fluctuation spectrum $S_s(q, \omega)$ in a hard-disk fluid ($A/A_0 = 2$) at $q\sigma = 6.1$, $N = 9$ kinetic model solution (full curve), single relaxation time approximation (dashed curve), and simulation data (circles).

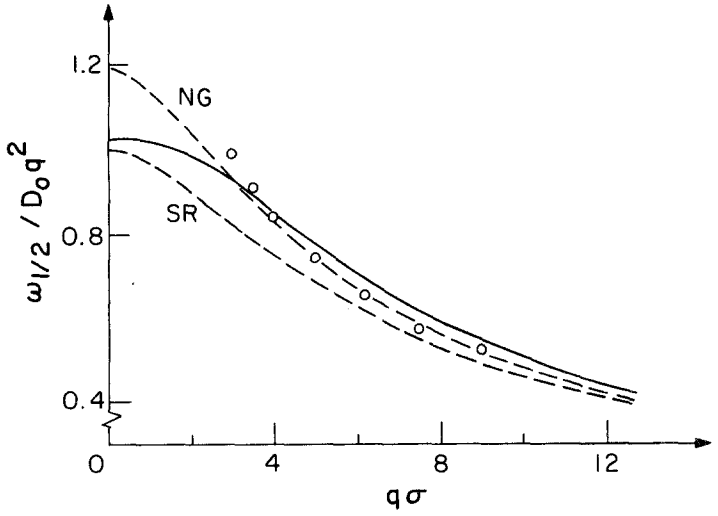

Fig. 4. Dimensionless half-width at half maximum of $S_s(q, \omega)$ in a hard-disk fluid ($A/A_0 = 2$), $N = 9$ kinetic model solution (full curve), single relaxation time approximation (SR), Nelkin–Ghatak model (NG), and simulation data (circles).

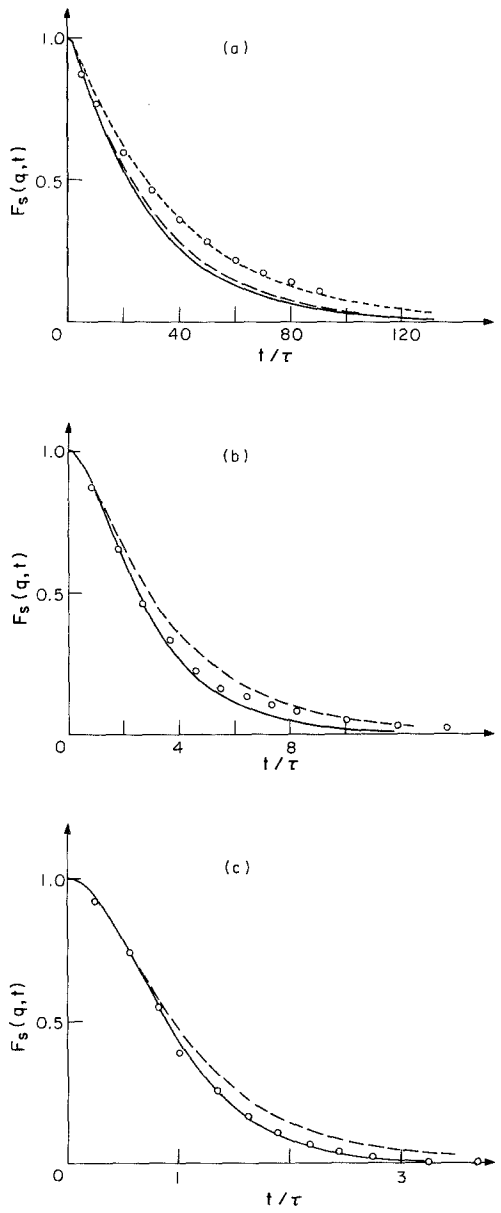

Fig. 5. The van Hove self-correlation function $F_s(q,t)$ in a hard-disk fluid ($A/A_0 = 1.4$), $N = 27$ kinetic model solution (full curve), Nelkin–Ghatak model with $D/D_0 = 0.775$ (dashed curve), single relaxation time approximation (longer dashed curve in (a)), and simulation data (circles). (a) $q\sigma = 3$, (b) $q\sigma = 11$, (c) $q\sigma = 25$.

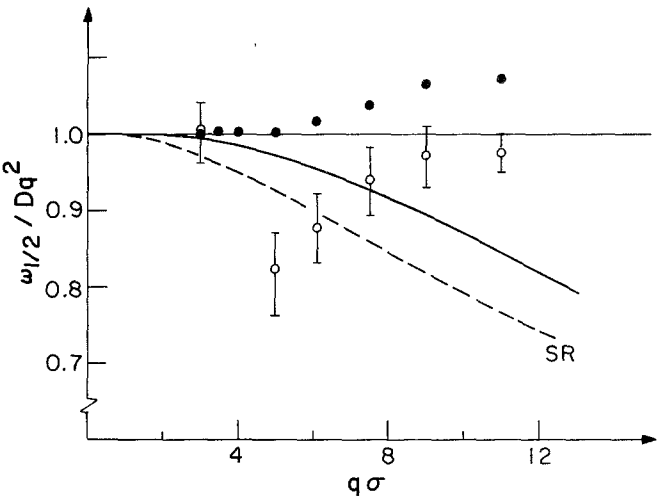

Fig. 6. Dimensionless half-width at half maximum of $S_s(q,\omega)$ in a hard-disk fluid ($A/A_0 = 14$), $N = 9$ kinetic model solution (full curve), single relaxation time approximation (dashed curve), Gaussian approximation (closed circles), and simulation data (open circles).

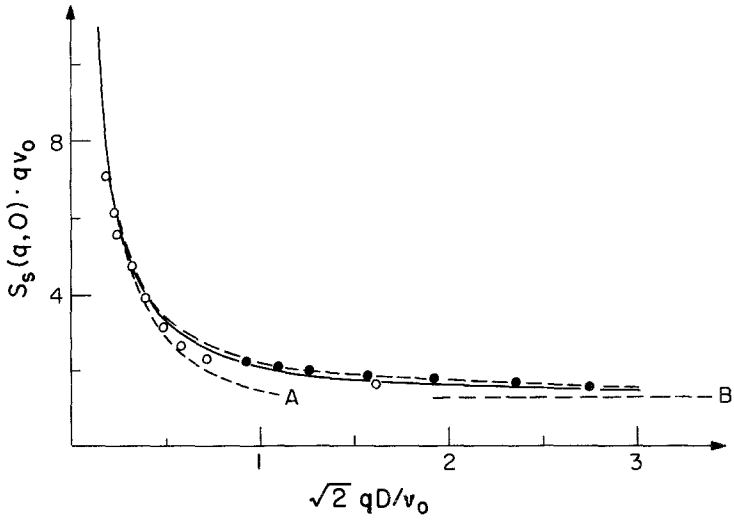

Fig. 7. Dimensionless peak height of $S_s(q,\omega)$ in a hard-disk fluid, $N = 9$ kinetic model solution (full curve), single relaxation time approximation and Nelkin–Ghatak model (dashed curve), and simulation data for $A/A_0 = 1.4$ (open circles) and $A/A_0 = 2$ (closed circles). Limiting results are hydrodynamic behavior v_0/qD (dashed curve A) and free particle behavior $(\pi/2)^{1/2}$ (dashed curve B).

which display a minimum in $\omega_{1/2}$ at $q\sigma \sim 5$, an effect that is entirely absent in the theoretical results. This behavior is well known in three-dimensional fluids with continuous potentials.[1] Its presence in a hard-core fluid further confirms the interpretation that the effect arises from strong spatial correlations between near neighbors. In Fig. 6 we also show the results corresponding to the Gaussian approximation which assumes

$$F_s(q,t) = \exp\left[-q^2\langle r^2(t)\rangle/4\right] \tag{11}$$

Since this approximation does not lead to a minimum in $\omega_{1/2}$, the width behavior can also be regarded as a higher-order effect beyond the second spatial moments of $G_s(r,t)$. It should be noted that in Fig. 6 the simulation data are normalized by D_{eff}, whereas the kinetic theory results are normalized by D_0. With $D_{\text{eff}}/D_0 = 0.775$ at $A/A_0 = 1.4$, a comparison of calculations and simulation with both normalized to the same D value would emphasize even more dramatically the inadequacy of the Enskog theory in a calculation without adjustable parameter. One can also discuss the peak height of $S_s(q,\omega)$ in a manner similar to Fig. 6. Figure 7 shows that the kinetic theory is able to provide a reasonable calculation of $S_s(q,0)$, even though it is unable to describe $\omega_{1/2}$.

ACKNOWLEDGMENTS

One of us (E.L.) would like to thank the Department of Nuclear Engineering at MIT for kind hospitality and financial support. This work was supported in part by the National Science Foundation and by the Army Research Office.

APPENDIX

Here we provide the explicit formulas for the complete orthonormal set of momentum functions and the general matrix elements of the Lorentz–Enskog collision operator and the free-particle correlation functions in this basis. The two-dimensional Sonine polynomial basis is defined[6] by

$$\Psi_{NM}(\zeta) = (-1)^N C_{NM} |\zeta|^M L_N^{|M|}(\zeta^2) e^{iM\varphi},$$
$$N = 0, 1, 2, \ldots, \quad M = 0, \pm 1, \pm 2, \ldots \tag{A.1}$$

with $C_{NM} = (N!/(N!+|M|!))^{1/2}$, $\bar{\zeta} = \boldsymbol{p}(2mT)^{1/2}$, $\zeta_x = \zeta \sin\varphi$, $\zeta_y = \zeta\cos\varphi$ and $L_n^m(x)$ are the Laguerre polynomials. They are normalized with respect to the scalar product:

$$\langle NM \mid N'M'\rangle = \int d\boldsymbol{\zeta}\, \Psi_{NM}^*(\zeta)\varphi(\zeta)\Psi_{N'M'}(\zeta) = \delta_{NN'}\delta_{MM'} \tag{A.2}$$

where $\varphi(\zeta) = (1/\pi)\exp(-\zeta^2)$ is the Maxwellian velocity distribution. The matrix elements of the Lorentz–Enskog operator are defined by

$$\langle NM|T^s|N'M'\rangle = -i\nu(2\pi)^{1/2}\int \frac{d\hat{r}}{2\pi}\int d\zeta_0\, d\zeta_1\, \varphi(\zeta_0)\varphi(\zeta_1)\theta(\zeta_{01}\cdot\hat{r}) \times (\zeta_{01}\cdot\hat{r})\Psi^*_{NM}(\zeta_0)\left[\Psi_{N'M'}(\zeta_0') - \Psi_{N'M'}(\zeta_0)\right] \quad \text{(A.3)}$$

Here, ν is the collision frequency and $\zeta_0' = \zeta_0 - (\zeta_{01}\hat{r})\hat{r}$ is the postcollision momentum of the tagged particle. The matrix elements may be easily obtained as a special case of the results previously derived.[6] Some general symmetry properties are helpful:

$$\langle NM|T^s|N'M'\rangle = \langle NM|T^s|N'M\rangle\delta_{MM'} \quad \text{(A.4a)}$$

$$\langle NM|T^s|N'M'\rangle = \langle N'M'|T^s|NM\rangle \quad \text{(A.4b)}$$

$$\langle N-M|T^s|N'-M\rangle = \langle NM|T^s|N'M\rangle \quad \text{(A.4c)}$$

where Eq. (A.4a) follows from rotational invariance. Because of Eq. (A.4c) we can assume $M > 0$ in the following. One finds

$$\langle NM|T^s|N'M\rangle = i\nu\left(\frac{1}{2}\right)^{N+N'+M}\left[\frac{(N+M)!}{N!}\,\frac{(N'+M)!}{N'!}\right]^{1/2} H^{(+)}(NN', M) \quad \text{(A.5a)}$$

with

$$H^{(+)}(NN', M) = \sum_m \frac{4m^2}{4m^2-1} K_m(NN', M) \quad \text{(A.5b)}$$

$$K_m(NN', M) = \sum_{nn'\nu\nu'}(-1)^{n+n'} \times \frac{(n+n'+|m+M|)!\,\Gamma(\nu+\nu'+|m|+3/2)/\Gamma(3/2)}{\nu!\,\nu'!\,n!\,n'!\,(\nu+|m|)!\,(\nu'+|m|)!\,(n+|m+M|)!\,(n'+|m+M|)!} \quad \text{(A.5c)}$$

with the summation restrictions $2(\nu+n)+|m|+|m+M| = 2N+M$ and $2(\nu'+n')+|m|+|m+M| = 2N'+M$.

The free-particle correlation functions are defined by

$$\langle NM|\tilde{\phi}^{(0)}(x)|N'M'\rangle = \int d\zeta \frac{\Psi^*_{NM}(\zeta)\varphi(\zeta)\Psi_{N'M'}(\zeta)}{(\hat{q}\cdot\zeta) - x} \quad \text{(A.6)}$$

where $\tilde{\phi}^{(0)}(x) = \sqrt{2}\, qv_0\phi^{(0)}(q,z)$ and $x = z/\sqrt{2}\, qv_0$. Due to rotational invariance, the set of all correlation functions can be divided into a longitudinal

and a transverse part. We are interested here in the longitudinal part which is coupled to the density correlation, and therefore define the longitudinal Sonine polynomials by

$$|NM\rangle_+ = \begin{cases} |NM\rangle & \text{for} \quad M = 0 \\ \dfrac{1}{\sqrt{2}}(|NM\rangle + |N - M\rangle) & \text{for} \quad M > 0 \end{cases} \tag{A.7}$$

By expanding the Sonine-polynomials Ψ_{NM} in terms of Hermite polynomials H_n we obtain the following results:

$$\begin{aligned} {}_+\langle NM|\tilde{\phi}^{(0)}(x)|N'M'\rangle_+ &= d_{MM'}(N!\,N'!\,(N+M)!\,(N'+M')!\,)^{1/2} \\ &\times \sum_{n_1} \frac{2^{n_1}}{n_1!\,n_2!\,n_2'!}\,\mathscr{C}(n_1 n_2 \,|\, NM)\,\mathscr{C}(n_1' n_2' \,|\, N'M')\,\phi_{n_2 n_2'}(x) \end{aligned} \tag{8a}$$

with

$$d_{MM'} = \begin{cases} 1 & \text{for} \quad M = M' = 0 \\ \sqrt{2} & \text{for} \quad M = 0 \quad \text{or} \quad M' = 0 \\ 2 & \text{for} \quad M \neq 0, \quad M' \neq 0 \end{cases} \tag{A.8b}$$

$$\begin{aligned} \mathscr{C}(n_1 n_2 \,|\, NM) = \frac{\Gamma((n_1+1)/2)/\Gamma(1/2)\cdot\Gamma((n_2+M+1)/2)/\Gamma(1/2)}{(N+M)!} \\ \times {}_3F_2\left(-\frac{M}{2}, -\left(\frac{M-1}{2}\right), \frac{n_1+1}{2}; \frac{1}{2}, \right. \\ \left. -\frac{(n_2+M-1)}{2}; 1\right) \end{aligned} \tag{A.8c}$$

$$\phi_{n_2 n_2'}(x) = H_{n_2}(x)H_{n_2'}(x)\varphi(x) - 2\sum_{n_3=|n_2-n_2'|}^{n_2+n_2'} A(n_2 n_2', n_3)\,g_{n_3}(x) \tag{A.8d}$$

$$A(n_2 n_2', n_3) = \frac{n_2!\,n_2'!\,2^{(n_2+n_2'-n_3)/2}}{((n_2+n_2'-n_3)/2)!\,((n_2+n_3-n_2')/2)!\,((n_2'+n_3-n_2)/2)!} \tag{A.8e}$$

and $g_n(x)$ are polynomials satisfying the same recursion relations as the Hermite polynomials $H_n(x)$.

$$g_{n+1}(x) = 2xg_n(x) - 2ng_{n-1}, \qquad n = 1, 2, \ldots \tag{A.8f}$$

with $g_0(x) = 0$, $g_1(x) = -1$. In Eq. (A.8a) $n_2 = 2N + M - n_1$, $n_{2'} = 2N' + M' - n_1$; in Eq. (A.8c) ${}_3F_2$ is a hypergeometric function[16]; and in Eq. (A.8d) $y(x) = i\sqrt{\pi}\,w(x)$ is the free-particle density correlation given in terms of the plasma dispersion function[17] $w(x)$.

REFERENCES

1. J. P. Hansen and I. R. McDonald, *Theory of Simple Liquids* (Academic Press, London, 1976); J-P. Boon and S. Yip, *Molecular Hydrodynamics* (McGraw-Hill, New York, 1980).
2. B. J. Alder and T. E. Wainwright, *Phys. Rev. Lett.* **18**:988 (1967); *J. Phys. Soc. Jpn. Suppl.* **26**:267 (1969); *Phys. Rev. A* **1**:18 (1970); T. E. Wainwright, B. J. Alder, and D. M. Gass, *Phys. Rev. A* **4**:233 (1971).
3. J. J. Erpenbeck and W. W. Wood, *Phys. Rev. A* **26**:1648 (1982).
4. J. R. Dorfman and E. G. D. Cohen, *Phys. Rev. Lett.* **25**:1257 (1970); *Phys. Rev. A* **6**:726 (1972), **12**:292 (1975); M. H. Ernst, E. H. Hauge, and J. M. J. van Leeuwen, *Phys. Rev. Lett.* **25**:1254 (1970); *Phys. Rev. A* **4**:2055 (1971). See also, J. R. Dorfman, in *Fundamental Problems in Statistical Mechanics*, E. G. D. Cohen, ed. (North Holland, Amsterdam, 1975), Vol. 3, p. 277; J. R. Dorfman, *Physica* **106A**:77 (1981).
5. Y. Pomeau and P. Resibois, *Phys. Rep.* **19**:63 (1975).
6. E. Leutheusser, S. Yip, E. J. Alder, and W. E. Alley, *J. Stat. Phys.* **35**:503 (1983).
7. E. P. Gross and E. A. Jackson, *Phys. Fluids* **2**:432 (1959).
8. M. Nelkin and A. Ghatak, *Phys. Rev.* **135A**:4 (1964).
9. S. Ranganathan and S. Yip, *Physics* **100A**:127 (1980).
10. I. M. de Schepper, M. H. Ernst, and E. G. D. Cohen, *J. Stat. Phys.* **25**:321 (1981).
11. D-P. Chou, Engineer's thesis, M.I.T. (1980).
12. M. L. Prueitt, Computer Simulation of Molecular Dynamics, Los Alamos Scientific Laboratory Report LA-4696 (1971).
13. B. J. Alder and T. E. Wainwright, *J. Chem. Phys.* **33**:1439 (1960); W. G. Hoover and B. J. Alder, *Ibid.* **46**:686 (1967).
14. B. J. Alder, D. M. Gass, and T. E. Wainwright, *J. Chem. Phys.* **53**:3813 (1970).
15. L. Verlet and D. Levesque, *Mol. Phys.* **46**:969 (1982).
16. M. Abramowitz and J. A. Stegun, *Handbook of Mathematical Functions* (Dover, New York, 1970).